Electron Spin Polarization Transfer from Photogenerated Spin-Correlated Radical Pairs to a Stable Radical Observer Spin

ARTICLE *in* THE JOURNAL OF PHYSICAL CHEMISTRY A · MAY 2013

Impact Factor: 2.69 · DOI: 10.1021/jp4045012 · Source: PubMed

THE JOURNAL OF PHYSICAL CHEMISTRY A

Article

pubs.acs.org/JPCA

Electron Spin Polarization Transfer from Photogenerated Spin-Correlated Radical Pairs to a Stable Radical Observer Spin

Michael T. Colvin, Raanan Carmieli, Tomoaki Miura, Sabine Richert, Daniel M. Gardner, Amanda L. Smeigh, Scott M. Dyar, Sarah M. Conron, Mark A. Ratner, and Michael R. Wasielewski*

Department of Chemistry and Argonne-Northwestern Solar Energy Research (ANSER) Center, Northwestern University, Evanston, Illinois 60208-3113, United States

Supporting Information

ABSTRACT: A series of donor–chromophore–acceptor–stable radical (D–C–A–R$^{\bullet}$) molecules having well-defined molecular structures were synthesized to study the factors affecting electron spin polarization transfer from the photogenerated D$^{+\bullet}$–C–A$^{-\bullet}$ spin-correlated radical pair (RP) to the stable radical R$^{\bullet}$. Theory suggests that the magnitude of this transfer depends on the spin–spin exchange interaction ($2J_{DA}$) of D$^{+\bullet}$–C–A$^{-\bullet}$. Yet, the generality of this prediction has never been demonstrated. In the D–C–A–R$^{\bullet}$ molecules described herein, D is 4-methoxyaniline (MeOAn), 2,3-dihydro-1,4-benzodioxin-6-amine (DioxAn), or benzobisdioxole aniline (BDXAn), C is 4-aminonaphthalene-1,8-dicarboximide, and A is naphthalene-1,8:4,5-bis(dicarboximide) (**1A,B**–**3A,B**) or pyromellitimide (**4A,B**–**6A,B**). The terminal imide of the acceptors is functionalized with either a hydrocarbon (**1A**–**6A**) or a 2,2,6,6-tetramethyl-1-piperidinyloxyl radical (R$^{\bullet}$) (**1B**–**6B**). Photoexcitation of C with 416-nm laser pulses results in two-step charge separation to yield D$^{+\bullet}$–C–A$^{-\bullet}$–(R$^{\bullet}$). Time-resolved electron paramagnetic resonance (TREPR) spectroscopy using continuous-wave (CW) microwaves at both 295 and 85 K and pulsed microwaves at 85 K (electron spin–echo detection) was used to probe the initial formation of the spin-polarized RP and the subsequent polarization of the attached R$^{\bullet}$ radical. The TREPR spectra show that $|2J_{DA}|$ for D$^{+\bullet}$–C–A$^{-\bullet}$ decreases in the order MeOAn$^{+\bullet}$ > DioxAn$^{+\bullet}$ > BDXAn$^{+\bullet}$ as a result of their spin density distributions, whereas the spin–spin dipolar interaction (d_{DA}) remains nearly constant. Given this systematic variation in $|2J_{DA}|$, electron spin–echo-detected EPR spectra of **1B**–**6B** at 85 K show that the magnitude of the spin polarization transferred from the RP to R$^{\bullet}$ depends on $|2J_{DA}|$.

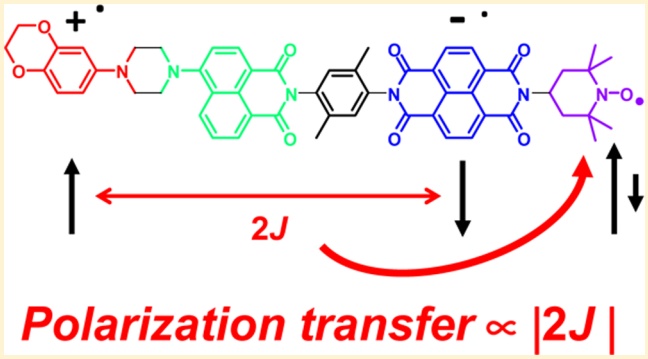

INTRODUCTION

Controlling the spin dynamics of multispin systems is a major goal in the quest for molecule-based spintronics.[1−4] A greater fundamental understanding of the factors controlling spin dynamics in complex, yet versatile organic multispin systems is necessary before construction of organic spintronic devices is feasible. This requires further exploration of structure–function relationships in organic systems that can create, store, and transfer spin information. Photoexcitation is known to produce well-defined initial spin states in organic molecules, so that much of the research directed toward this goal has focused on controlling the spin dynamics of photogenerated multispin systems. In the simplest case, photoexcitation of organic molecules to their lowest excited singlet states often results in spin-selective intersystem crossing to produce highly spin-polarized triplet states.[5] Spin polarization can also be created by spin state mixing in multispin systems; for example, triplet–doublet mixing has received significant attention in systems in which the spin–spin exchange interaction ($2J$) varies, including systems based on diffusing noncovalent molecular species, coordinatively linked systems, and systems covalently bound by flexible linkers.[6−13] Recent studies on covalent radical–chromophore systems with well-defined distances and orientations have demonstrated that the photophysical pathways and spin dynamics of these systems depend on both the overall electronic and spin–spin exchange couplings between the radical and the photoexcited chromophore.[14−18] Finally, photoinitiated electron transfer within covalently linked organic donor–bridge–acceptor (D–B–A) molecules can produce highly polarized spin-correlated radical pairs (RPs) in which the initial spin state is well-defined and the magnetic interactions between the two radicals are relatively weak.[19−25]

Following rapid charge separation, the initially formed singlet RP, ^{1}(D$^{+\bullet}$–B–A$^{-\bullet}$), undergoes radical-pair intersystem crossing (RP-ISC)[26,27] induced by electron–nuclear hyperfine coupling within the radicals to produce the triplet RP, ^{3}(D$^{+\bullet}$–B–A$^{-\bullet}$). The charge-recombination (CR) reactions are spin-selective, such that RP-ISC can be a kinetic bottleneck

Received: May 6, 2013
Revised: May 25, 2013
Published: May 30, 2013

for the overall CR process.[28] Application of an external magnetic field has been shown to dramatically change the spin-selective CR reaction yields.[22,28,29] These magnetic field effects (MFEs) allow control over the CR rates, so that both the spin-dependent CR pathways and the RP spin−spin exchange interaction, $2J = E_S - E_T$, where E_S and E_T are spin state energies for the singlet and triplet RP states, respectively, can be probed. The value of $2J$ depends exponentially on distance and is proportional to the square of the electronic coupling matrix element for charge recombination (V_{CR}^2).[30,31] It is also possible to control the RP spin dynamics on a nanosecond time scale by photogenerating the RP in an applied magnetic field and applying a resonant microwave (MW) pulse that inverts the spins of the RP, thus controlling the yields of the singlet and triplet products from CR. This technique is known as reaction-yield-detected magnetic resonance (RYDMR)[32,33] and has been shown, for example, to increase the photogenerated RP lifetime in bacterial photosynthetic reaction center proteins by 1−2 orders of magnitude.[34]

At the ∼350 mT magnetic field characteristic of time-resolved EPR (TREPR) measurements at X-band, the triplet sublevels of $^3(D^{+\bullet}-B-A^{-\bullet})$ undergo Zeeman splitting and are best described by the T_{+1}, T_0, and T_{-1} eigenstates that are quantized along the applied magnetic field, whereas the $^1(D^{+\bullet}-B-A^{-\bullet})$ (S) energy is unaffected.[20,25,35,36] Generally, when $2J_{DA}$ is <10 mT, coherent S-T_0 mixing occurs, and the resulting two mixed states are preferentially populated due to the initial population of the singlet precursor, so that the four EPR transitions that occur between these mixed states and the initially unpopulated T_{+1} and T_{-1} states are spin-polarized.[26,27] The TREPR spectrum consists of two antiphase doublets, centered at the g factors of the individual radicals that comprise the pair, in which the splitting of each doublet is determined by $2J_{DA}$. The electron spin polarization pattern from low field to the high field of the EPR signal [i.e., which transitions are in enhanced absorption (a) or emission (e)] is determined by the sign rule:[37] $\Gamma = \mathrm{sign}\{\mu[J_{DA} - d_{DA}(3\cos^2\theta - 1)]\}$, where μ is −1 or +1 for a singlet or triplet excited-state precursor, respectively; d_{DA} is the spin−spin dipolar coupling between $D^{+\bullet}$ and $A^{-\bullet}$; and θ is the angle between a vector joining the centers of the spin density distributions on each radical of the RP and a vector along the external applied magnetic field direction. If Γ is negative, the spin polarization pattern is (e, a, e, a), whereas if Γ is positive, the spin polarization pattern is (a, e, a, e). For example, if the RP precursor is a singlet excited state, $2J_{DA} > 0$, and d_{DA} is averaged to zero in solution, Γ is negative, resulting in an (e, a, e, a) pattern. If the g factors of the two radicals are similar and/or are split by hyperfine couplings, the two doublets will overlap strongly and will appear as distorted (e, a) or (a, e) signals. The lifetime of the observed RP spin polarization is typically limited by the sum of the rates of spin−lattice relaxation ($1/T_1$) and population decay resulting from charge recombination ($1/\tau_{CR}$). Achieving greater control of the spin polarization lifetimes, particularly by extending them, is an important goal for spintronic information processing.

The subsequent charge recombination process is spin-selective; that is, $^1(D^{+\bullet}-B-A^{-\bullet})$ recombines to the singlet ground state, whereas $^3(D^{+\bullet}-B-A^{-\bullet})$ recombines to yield a neutral triplet $^3*(D-B-A)$ that acquires the non-Boltzmann spin population of the triplet RP state, provided that the energy of $^3(D^{+\bullet}-B-A^{-\bullet})$ is greater than that of $^3*(D-B-A)$.[38] The spin polarization pattern of the six EPR transitions of $^3*(D-B-A)$ at the canonical (x, y, z) orientations relative to that of the applied magnetic field can be used to determine the mechanism of $^3*(D-B-A)$ formation. When an RP undergoes ISC by S−T_0 mixing, subsequent charge recombination to the neutral triplet yields the characteristic (a, e, e, a, a, e) polarization pattern (low field to high field), whereas spin−orbit intersystem crossing produces a variety of other patterns characteristic of selective population of the low-field eigenstates of the triplet.[38]

Recently, structure−function relationships of photogenerated RPs within D−B−A molecules have received significant attention.[19,20,25,35,39] These studies have found that the $2J_{DA}$ and d_{DA} values between the two unpaired spins $D^{+\bullet}$ and $A^{-\bullet}$ affect multiple aspects of the photophysics and spin dynamics in these systems, including the radical pair intersystem crossing (RP-ISC) rate,[30] the triplet sublevels that mix with the singlet state,[15] the charge recombination pathways,[40,41] and the spectral line shape and intensity of the RP TREPR spectra.[25] Thus, it is reasonable to consider what roles $2J_{DA}$ and d_{DA} play in the photophysics and spin dynamics observed in photogenerated triradicals. However, structure−function relationships in triradicals have not been examined at a wide variety of time scales and interaction strengths. This information is best obtained by utilizing both time-resolved optical absorption and TREPR spectroscopies. There are several mechanisms that can account for the transfer of spin polarization from $D^{+\bullet}-B-A^{-\bullet}$ to $R^\bullet$ in a $D^{+\bullet}-B-A^{-\bullet}-R^\bullet$ system, namely (i) triplet−doublet mixing between $^3*A$ and $R^\bullet$ following charge recombination of $D^{+\bullet}-B-A^{-\bullet}$ to yield $D-B-^3*A-R^\bullet$; (ii) spin−spin exchange and dipolar coupling between the proximate $A^{-\bullet}$ and $R^\bullet$ radicals; and (iii) polarization transfer from $D^{+\bullet}-B-A^{-\bullet}$ to $R^\bullet$, which is predicted to depend on both $2J_{DA}$ and d_{DA} in $D^{+\bullet}-B-A^{-\bullet}$.

The interaction of a stable radical with a photogenerated spin-correlated RP was initially studied in bacterial photosynthetic reaction center proteins.[42−45] Photoexcitation of the primary bacteriochlorophyll dimer electron donor (P) in the reaction center protein leads to reduction of a nearby bacteriopheophytin electron acceptor (I) in about 3 ps to produce the $P^{+\bullet}-I^{-\bullet}$ spin-correlated RP.[46] If the secondary quinone electron acceptor (Q) in this protein is chemically reduced to $Q^{-\bullet}$ prior to the formation of $P^{+\bullet}-I^{-\bullet}$, photogeneration of $P^{+\bullet}-I^{-\bullet}$ has been shown to spin polarize this nearby $Q^{-\bullet}$ "observer spin". The formation of quartet and excited doublet states within the $P^{+\bullet}-I^{-\bullet}-Q^{-\bullet}$ triradical is not observed because the spin−spin exchange interaction between $I^{-\bullet}$ and $Q^{-\bullet}$ ($2J_{IQ}$) is relatively weak.[42−45] Interestingly, theoretical investigations of this phenomenon predict that electron spin polarization of $Q^{-\bullet}$ in the triradical depends on the sign and magnitude of the spin−spin exchange interaction between $P^{+\bullet}$ and $I^{-\bullet}$ in the photogenerated RP ($2J_{PI}$) and the singlet and the triplet RP charge recombination rates, k_S and k_T, respectively,[44,45] among other factors; however, the generality of this prediction has not been investigated experimentally because the values of $2J_{PI}$ and $2J_{IQ}$ within photosynthetic reaction center proteins cannot be readily changed systematically. Fortunately, the advent of covalent, fixed-distance multistep electron donor−acceptor molecules makes it possible to design systems in which all of the magnetic parameters of the photogenerated $D^{+\bullet}-B-A^{-\bullet}-R^\bullet$ triradical, including $2J_{DA}$, $2J_{AR}$, d_{DA}, and d_{AR}, can be varied in a controlled fashion. For example, we recently examined the photophysics and spin dynamics of photogenerated triradicals in which nitroxides were covalently bound to either the bridge or acceptor in D−B−A molecules.[47−50] We found that the presence of a third spin has

dx.doi.org/10.1021/jp4045012 | J. Phys. Chem. A 2013, 117, 5314−5325

almost no effect on the charge separation rates but, in some cases, slightly alters the charge recombination rates and results in spin polarization of the nitroxide radical coincident with the RP charge recombination reaction, indicating that the two processes are connected.

In contrast to the reaction center RP, several molecules have been examined in which $2J_{DA}$ and $2J_{AR}$ are large enough that quartet states and excited doublet states are observed following charge recombination.[51,52] A theoretical treatment of these systems suggests that the spin polarization is initially created within the photogenerated triradical, rather than from triplet−doublet interactions following charge recombination.[53] The mechanism of spin polarization of the stable radical is attributed to fluctuations in $2J_{DA}$ within the RP resulting from motions of the two radicals comprising the RP,[53] so that the predicted line shapes of the polarized stable radical in both the presence and absence of the photogenerated RP are similar.

Here, we report a study of the photophysics and spin dynamics of a series of donor−chromophore−acceptor−stable radical systems (D−C−A−R$^{\bullet}$) in which the chromophore acts as the primary electron acceptor following photoexcitation. The donors are 4-methoxyaniline (MeOAn), 2,3-dihydro-1,4-benzodioxin-6-amine (DioxAn), or benzobisdioxole aniline (BDXAn) attached to a 4-aminonaphthalene-1,8-dicarboximide (C) chromophore, which is, in turn, covalently attached through a 2,5-dimethylphenyl spacer to an imide nitrogen atom of either a naphthalene-1,8:4,5-bis(dicarboximide) (NI) (**1A,B**−**3A,B**) or a pyromellitimide (PI) acceptor (**4A,B**−**6A,B**) (see Chart 1). The remaining imide nitrogen atom of the NI or PI acceptor is terminated with either a hydrocarbon (**1A**−**6A**) or 2,2,6,6-tetramethyl-1-piperidinyloxyl (R$^{\bullet}$) (**1B**−**6B**). ^{3}*NI is energetically accessible by charge recombination of D$^{+\bullet}$−C−A$^{-\bullet}$ within **1A,B**−**3A,B**, whereas ^{3}*PI is inaccessible within **4A,B**−**6A,B**, which provides a probe of whether the neutral triplet state (^{3}*A) formed by charge recombination plays a role in transferring polarization to R$^{\bullet}$. We chose R$^{\bullet}$ because it cannot be reduced by A$^{-\bullet}$ photogenerated in the D−C−A−R$^{\bullet}$ systems. A spin-correlated RP pair is observed in **1A**−**6A** and **1B**−**6B** following photoinitiated charge separation, whereas spin polarization on R$^{\bullet}$ appears in **1B**−**6B**. By comparing the spin dynamics in liquid and solid solutions, we are able to distinguish the contributions of $2J_{DA}$ and d_{DA}. The dipolar interaction within the RP, d_{DA}, is inherently anisotropic and is essentially averaged to zero in liquid solution, whereas $2J_{DA}$ is isotropic under all conditions, so that $2J_{DA}$ should, in large part, account for the polarization observed in liquid solution at 295 K. Moreover, because $d_{DA} \propto 1/r^3$ whereas $2J_{DA} \propto e^{-r}$, the relatively small D−A distance changes within the **1A,B**−**6A,B** series result in d_{DA} remaining nearly constant, whereas $2J_{DA}$ varies by 1−2 orders of magnitude within the **1A,B**−**3A,B** and **4A,B**−**6A,B** series.

Pulsed EPR experiments provide a means of quantifying the degree of photogenerated polarization relative to the Boltzmann spin polarization and show that the degree of light-induced polarization depends on $|2J_{DA}|$. The role of the initial Boltzmann population of the radical is investigated by applying a π microwave pulse prior to photoexcitation to invert the spin sublevel population on R$^{\bullet}$. This initial inversion has a negligible effect on the transient polarization, demonstrating that the polarization is mostly due to $2J_{DA}$ within the RP. Polarization transfer from the RP to R$^{\bullet}$ provides a potential means to examine the properties of charge-separated states that are either too short-lived or too strongly coupled to be observed by TREPR and thus provides an additional method to probe the electronic coupling between D$^{+\bullet}$ and A$^{-\bullet}$ within donor−bridge−acceptor systems. It also provides a way to store photogenerated electron spin polarization for longer times than are typical of RPs, which can be tuned by altering the properties of the donor, acceptor, and radical, opening the possibility of using photogenerated electron spin polarization for information storage in spintronic devices.

Chart 1

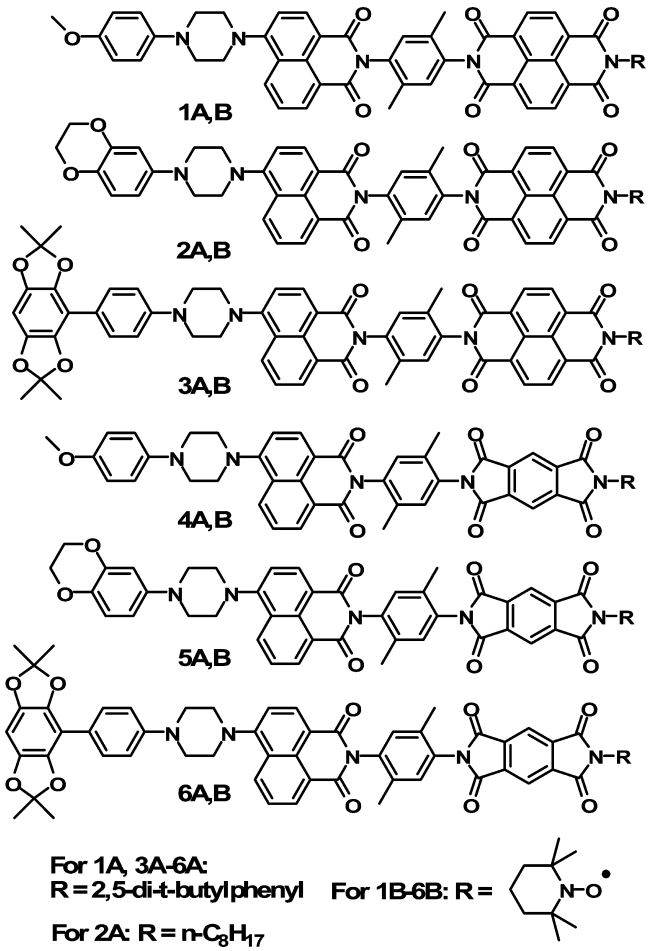

EXPERIMENTAL SECTION

Synthesis. The syntheses of **1** and **4** have been reported previously,[49] whereas the syntheses of **2**, **3**, **5**, and **6** are described in detail in the Supporting Information. Samples were purified on a silica column with 7% acetone in dichloromethane as the eluent, followed by preparative thin layer chromatography with the same eluent immediately prior to measurement, and were stored at −18 °C when not being used. All solvents for spectroscopy were spectrophotometric grade or distilled immediately prior to use.

Optical Spectroscopy. Ground-state absorption measurements were performed on a Shimadzu (UV-1800) spectrophotometer. The optical density of all samples was maintained between 0.1 and 0.6 at 416 nm, for both femtosecond and nanosecond transient absorption spectroscopy. Femtosecond transient absorption measurements were performed using the 416-nm, 110-fs output from the frequency-doubled output of a Ti:sapphire regenerative amplifier using techniques described earlier.[54] Samples were placed in a 2-mm-path-length glass

dx.doi.org/10.1021/jp4045012 | J. Phys. Chem. A 2013, 117, 5314−5325

cuvette. The samples were irradiated with 1.0 μJ per pulse focused to a 200-μm spot. The total instrument response function (IRF) for the pump−probe experiments was 180 fs. Samples for nanosecond transient absorption spectroscopy were placed in a 10-mm-path-length quartz cuvette equipped with a vacuum adapter and subjected to five freeze−pump−thaw degassing cycles. The samples were excited at 416 nm (1 mJ/pulse, 7 ns, 10 Hz) using the frequency-tripled output from a Spectra Physics Quanta-Ray Lab 150 Nd:YAG laser pumping a Spectra Physics Basi-scan optical parametric oscillator (OPO). The excitation pulse was focused to a 5-mm-diameter spot and matched to the diameter of the probe pulse generated using a xenon flashlamp (EG&G Electro-Optics FX-200). The signal was detected using a photomultiplier tube with high voltage applied to only four dynodes (Hamamatsu R928). The total instrument response time was 7 ns and was determined primarily by the laser pulse duration. Transient absorption kinetics were fit to a sum of exponentials convoluted with a Gaussian instrument function using Levenberg−Marquardt least-squares fitting.

EPR Spectroscopy. EPR measurements at X-band (9.5 GHz) were performed using a Bruker Elexsys E580 EPR spectrometer outfitted with a variable-Q dielectric resonator (ER-4118X-MD5-W1). Samples of **1A,B**−**6A,B** were prepared as toluene solutions (~10^{-4} M), loaded into quartz tubes (4 mm o.d. × 2 mm i.d.), subjected to five freeze−pump−thaw degassing cycles on a vacuum line (10^{-4} mbar), and sealed using a hydrogen torch. The EPR samples were stored in a freezer in the dark when not being used.

Continuous-wave (CW) EPR spectra were recorded at X-band using 0.2−2 mW microwave power and 0.01−0.05 mT field modulation at 100 kHz. TREPR measurements were performed using CW microwaves with direct detection. The temperature was controlled by an Oxford Instruments CF935 continuous-flow cryostat using liquid N_2. Samples of **1A,B**−**6A,B** were photoexcited at 416 nm (1.2 mJ/pulse, 7 ns, 10 Hz) using the frequency-tripled output from a Spectra Physics Quanta-Ray Pro 350 Nd:YAG laser pumping a Spectra Physics Basi-scan OPO. Following photoexcitation, kinetic traces of the transient magnetization were accumulated under CW microwave irradiation (2−20 mW). The field modulation was disabled to achieve an instrument response function (IRF) of $Q/\pi\nu \approx 30$ ns, where Q is the quality factor of the resonator and ν is the resonant frequency, whereas microwave signals in emission (e) and/or enhanced absorption (a) were detected in both the real and the imaginary channels (quadrature detection). Sweeping the magnetic field gave two-dimensional spectra versus both time and magnetic field. For each kinetic trace, the signal acquired prior to the laser pulse was subtracted from the data. Kinetic traces recorded at magnetic field values off-resonance were considered to be background signals, whose average was subtracted from all kinetic traces. The spectra were subsequently phased into a Lorentzian part and a dispersive part, and the former, also known as the imaginary magnetic susceptibility χ'', is presented.

Field-swept, echo-detected (FS-ED) EPR spectra were recorded at 85 K. The resonator was fully overcoupled for all pulsed experiments (Q < 200). The spin echo was generated using a two-pulse echo sequence following the laser pulse (laser−t_L−π/2−τ−π−τ−echo) where t_L = 1 μs and τ = 140 ns, and the π/2 and π microwave pulses were 12 and 24 ns long, respectively. After the transient species is generated by the laser pulse, the integrated echo intensity is recorded as a function of magnetic field to yield the spectrum at a given time after the laser pulse. Experiments with a π pulse preceding the laser pulse were carried out using the sequence (π−t_I−laser−t_L−π/2−τ−π−τ−echo), where t_I = 10 ns and the remaining parameters are the same. The spin-polarized EPR spectra were simulated with home-written MATLAB[55] programs using published models.[44,45,56]

Theory. Electron spin polarization transfer from a spin-correlated RP to a stable radical has been investigated in photosynthetic reaction centers both experimentally and theoretically.[42−45] A brief summary of the spin polarization transfer model[45] used to analyze the TREPR spectra is presented here. Photogeneration of the RP in the presence of the stable radical results in a triradical having spin dynamics that depend on the external magnetic field, B_0; the applied microwave field, B_1; and the exchange and dipolar interactions among the three paramagnetic species. These interactions can be described by the spin Hamiltonian in the rotating frame, given by

$$\begin{aligned}\mathcal{H}_{\mathrm{DAR}^\bullet} = \hbar[&(\omega_D - \omega_0)\mathbf{S}_{D_Z} + (\omega_A - \omega_0)\mathbf{S}_{A_Z} \\ &+ (\omega_{T^\bullet} - \omega_0)\mathbf{S}_{R^\bullet{}_Z} + A_{DA}\mathbf{S}_{D_Z}\mathbf{S}_{A_Z} + B_{DA} \\ &(\mathbf{S}_{D_X}\mathbf{S}_{A_X} + \mathbf{S}_{D_Y}\mathbf{S}_{A_Y}) + A_{AR^\bullet}\mathbf{S}_{A_Z}\mathbf{S}_{R^\bullet{}_Z} \\ &+ B_{AR^\bullet}(\mathbf{S}_{A_X}\mathbf{S}_{R^\bullet{}_X} + \mathbf{S}_{A_Y}\mathbf{S}_{R^\bullet{}_Y}) + \omega_1(\mathbf{S}_{D_X} + \mathbf{S}_{A_X} + \mathbf{S}_{R^\bullet{}_X})]\end{aligned} \tag{1}$$

where $\omega_i = g_i\beta_e B_0$ is the Zeeman frequency of the spins i, $j \in \{D^{+\bullet}, A^{-\bullet}, R^\bullet\}$, where D represents the donor, A the acceptor, and $R^\bullet$ the radical; ω_0 is the microwave frequency; $\mathbf{S}_i$ and $\mathbf{S}_j$ are the spin operators for the ith and jth electrons, respectively; and $\omega_1 = g_i\beta B_1$ is the angular momentum representation of the applied microwave field strength along the $+X$ direction. A_{ij} and B_{ij} are the secular and pseudosecular couplings between the ith and jth spins, given by

$$A_{ij} = -2J_{ij} + 2d_{ij} \tag{2}$$

$$B_{ij} = -2J_{ij} - d_{ij} \tag{3}$$

where $2J_{ij}$ is the isotropic spin−spin exchange interaction and d_{ij} is the dipole−dipole interaction between the relevant spins. Direct couplings between $D^{+\bullet}$ and $R^\bullet$ are neglected here because of the long distances between the two spins in **1B**−**6B**. At the magnetic fields typical for our experiments, the hyperfine interaction is not expected to substantially alter the spin polarization pattern and was neglected to simplify the analysis.

To simulate the TREPR spectra, the Liouville equation of motion for the three-spin Hamiltonian is solved numerically[45]

$$\begin{aligned}\frac{\partial\rho}{\partial\tau} = &-\frac{\mathrm{i}}{\hbar}[\mathcal{H}_{\mathrm{DAR}^\bullet}, \rho_{\mathrm{DAR}^\bullet}] - \frac{k_S}{2}(\mathbf{P}_S\rho_{\mathrm{DAR}^\bullet} + \rho_{\mathrm{DAR}^\bullet}\mathbf{P}_S) \\ &- \frac{k_T}{2}(\mathbf{P}_T\rho_{\mathrm{DAR}^\bullet} + \rho_{\mathrm{DAR}^\bullet}\mathbf{P}_T) - \mathbf{W}\rho_{\mathrm{DAR}^\bullet}\end{aligned} \tag{4}$$

Here, the first term describes the spin dynamics induced by the spin Hamiltonian, whereas the second and third terms describe the charge recombination of the singlet and triplet RPs with rate constants k_S and k_T, respectively, where $\mathbf{P}_S$ and $\mathbf{P}_T$ denote the projection operators of the singlet and triplet states, respectively, of the spin-correlated RP, and $\mathbf{W}$ describes the longitudinal (T_1) and tranverse (T_2) spin relaxation processes for each of the three spins. The spin dynamics of $R^\bullet$ generated

dx.doi.org/10.1021/jp4045012 | J. Phys. Chem. A 2013, 117, 5314−5325

by the spin-selective recombination processes is simultaneously calculated by another Liouville equation in the doublet subspace as

$$\frac{\partial \rho_{R^\bullet}}{\partial t} = -\frac{i}{\hbar}[\mathcal{H}_{R^\bullet}, \rho_{R^\bullet}] - \mathbf{W}\rho_{R^\bullet} + \mathrm{tr}_{DA}\left[\frac{k_S}{2}(\mathbf{P}_S\rho_{DAR^\bullet} + \rho_{DAR^\bullet}\mathbf{P}_S) + \frac{k_T}{2}(\mathbf{P}_T\rho_{DAR^\bullet} + \rho_{DAR^\bullet}\mathbf{P}_T)\right] \quad (5)$$

where

$$\mathcal{H}_{DAR^\bullet} = \hbar(\omega_{R^\bullet} - \omega_0)\mathbf{S}_{R^\bullet_Z} + \hbar\omega_1\mathbf{S}_{R^\bullet_X} \quad (6)$$

The total EPR signal, I_{B_0}, at each magnetic field point, B_0, is calculated by a simple sum of the Y components of the magnetization as

$$I_{B_0} \propto \mathrm{tr}[(\mathbf{S}_{D_Y} + \mathbf{S}_{A_Y} + \mathbf{S}_{R^\bullet_Y})\rho_{DAR^\bullet}] + \mathrm{tr}(\mathbf{S}_{R^\bullet_Y}\rho_{R^\bullet}) \quad (7)$$

The isotropic g factors used in the simulations were determined from CW-EPR spectra of the respective radicals (see the Supporting Information). Inhomogeneous broadening was added by convoluting the spectra with a Gaussian line shape function. The calculated spectra were fit to the experimental data by optimizing the two exchange interactions, $2J_{DA}$ and $2J_{AR}$, and the charge recombination rates from the singlet and triplet radical pair states. The fitting parameters are listed in Table S1 (Supporting Information). The spin dynamics of ^{3}*NI formed following charge recombination within **1B**−**3B** and its interaction with R$^\bullet$ were not taken into account.

RESULTS

Radical Ion Pair Energy Levels. The one-electron redox potentials of the donors and acceptors used to calculate the free energies of the charge-separated states in **1A,B**−**6A,B** in toluene at 295 K are as follows (all versus SCE): MeOAn (E_{OX} = 0.79 V),[57] DioxAn (E_{OX} = 0.62 V), BDXAn (E_{OX} = 0.83 V),[39] C (E_{RED} = −1.41 V),[57] PI (E_{RED} = 0.71 V),[58] and NI (E_{RED} = −0.53 V).[57] We previously showed that attachment of R$^\bullet$ to NI and PI does not alter their redox potentials.[49] Given that photoexcitation of D−C, where D = MeOAn, DioxAn, and BDXAn results in quantitative charge separation to produce D$^{+\bullet}$−C$^{-\bullet}$ with spectroscopically determined energies of 2.48, 2.31, and 2.51 eV, respectively, in toluene,[39,57] the energy levels for the charge-separated states, D$^{+\bullet}$−C−A$^{-\bullet}$, were determined in toluene using the equation

$$\Delta G_F = \Delta G_I + \mathrm{sign}(E_I - E_F) + \frac{e^2}{\varepsilon_S}\left(\frac{1}{r_I} - \frac{1}{r_F}\right)$$
$$\text{if } |E_F| > |E_I|, \quad \text{then sign} = (-)$$
$$\text{where}$$
$$\text{if } |E_I| > |E_F|, \quad \text{then sign} = (+) \quad (8)$$

where ΔG_I and ΔG_F are the energies above the ground state for the initial and final ion pairs, respectively; E_I and E_F are the redox potentials for the initial and final ions, respectively, between which the electron is transferred; r_I and r_F are the initial and final ion pair distances, respectively; e is the electronic charge; and ε_S is the static dielectric constant of the solvent (ε_S = 2.38 for toluene). The distances r_I and r_F between the donor, bridge, and acceptor components were determined from the energy-minimized structures of D−C−A using MM+ force field calculations.[59] The calculated values of $\Delta G_{RP} = \Delta G_F$ are reported in Table 1. The corresponding lowest triplet state energies (E_T) of NI, C, and PI are 2.03, 2.05, and 2.45 eV, respectively.[47,49] In a glassy organic solvent at cryogenic temperatures, ΔG_{RP} increases by about 0.2 eV relative to that in liquid toluene at room temperature resulting from loss of solvent motion.[21,60] Thus, $\Delta G_{RP} \geq E_T$ for the donors and acceptors comprising **1A,B**−**3A,B**, whereas $\Delta G_{RP} \leq E_T$ for the donors and acceptors comprising **4A,B**−**6A,B**.

Table 1. Radical Ion Pair Distance and Energies at 295 K

molecules	D$^{+\bullet}$−C$^{-\bullet}$−A distance (Å)	D$^{+\bullet}$−C−A$^{-\bullet}$ distance (Å)	ΔG_{RP} (eV)
1A,B	7.7	20	2.08
2A,B	8.9	21	1.83
3A,B	13.1	26[a]	1.86
4A,B	7.7	19	2.21
5A,B	8.9	20	1.98
6A,B	13.1	25[a]	2.03

[a]Determined experimentally using out-of-phase electron spin−echo envelope modulation (OOP-ESEEM) (see ref 39 and Figure S6 of the Supporting Information).

Transient Optical Absorption Spectroscopy. The ground-state absorption spectra of **2B** and **5B** are shown in Figure 1. The corresponding spectra of the remaining molecules in the series **1A,B**−**6A,B** are very similar. The spectrum of C has been described in detail previously and exhibits a charge-transfer band centered at 397 nm in toluene.[47,57] In addition to the charge-transfer band, **1A,B**−**3A,B** show additional absorption bands at 343, 363, and 382 nm due to π−π^* transitions in the NI acceptor, whereas for **4A,B**−**6A,B**, no significant contribution from the PI acceptor or R$^\bullet$ is observed at λ > 350 nm.

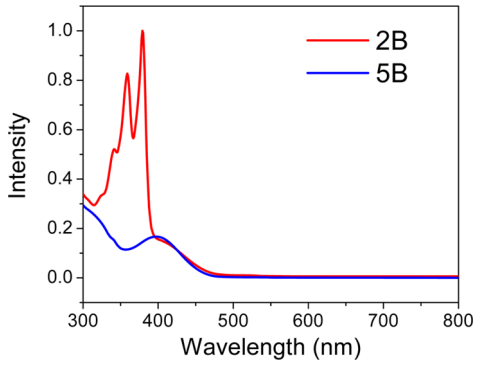

Figure 1. Steady-state absorption spectra of **2B** and **5B** in toluene.

Femtosecond and nanosecond transient absorption spectra of **1A,B**−**6A,B** were acquired in toluene to examine what effect, if any, the presence of R$^\bullet$ has on the charge separation and recombination time constants. Photoexcitation of C into its charge-transfer band at 416 nm results in the reaction D−^{1}*C−A−(R$^\bullet$) → D$^{+\bullet}$−C$^{-\bullet}$−A−(R$^\bullet$), where oxidation of D = MeOAn, DioxAn, or BDXAn occurs with $\tau_{CS1} \leq 15$ ps in all cases (Table 2). The initial charge separation is followed by the appearance of an absorption band at 480 nm in **1A,B**−**3A,B** or 720 nm in **4A,B**−**6A,B** indicative of NI$^{-\bullet}$ or PI$^{-\bullet}$ formation, respectively, so that the overall charge separation is a two-step

dx.doi.org/10.1021/jp4045012 | J. Phys. Chem. A 2013, 117, 5314−5325

Table 2. Time Constants for Charge Separation and Recombination at 295 K, $2J_{DA}$ at 295 and 85 K, and d_{DA} at 85 K

				$2J_{DA}$ (mT)		d_{DA} (mT)
molecule	τ_{CS1} (ps)	τ_{CS2} (ps)	τ_{CR} (ns)	295 K	85 K	85 K
1A	9.8 ± 0.5	430 ± 20	210 ± 5	2.0 ± 0.2	0.5 ± 0.1	−0.30 ± 0.02
1B	7.0 ± 0.5	400 ± 20	506 ± 10	1.8 ± 0.2	–	–
2A	5.2 ± 0.4	434 ± 5	260 ± 11	0.35 ± 0.03	0.07 ± 0.02	−0.25 ± 0.02
2B	6.0 ± 0.5	560 ± 50	240 ± 11	0.50 ± 0.03	–	–
3A	13.0 ± 2.5	300 ± 20	200 ± 60	0.25 ± 0.02	0.002 ± 0.001	−0.18 ± 0.02
3B	12.5 ± 0.6	320 ± 16	180 ± 15	0.20 ± 0.02	–	–
4A	6.9 ± 0.5	5000 ± 500	73 ± 2	1.5 ± 0.02	0.4 ± 0.1	−0.30 ± 0.02
4B	8.0 ± 0.5	3500 ± 500	109 ± 3	1.7 ± 0.02	–	–
5A	6.2 ± 1.6	2800 ± 200	100 ± 3	0.3 ± 0.02	0.09 ± 0.02	−0.24 ± 0.02
5B	6.6 ± 0.3	2800 ± 200	110 ± 3	0.20 ± 0.03	–	–
6A	15.6 ± 0.5	4000 ± 300	148 ± 3	0.12 ± 0.01	−0.003 ± 0.001	−0.16 ± 0.02
6B	14.1 ± 0.5	4000 ± 200	220 ± 2	0.17 ± 0.01	–	–

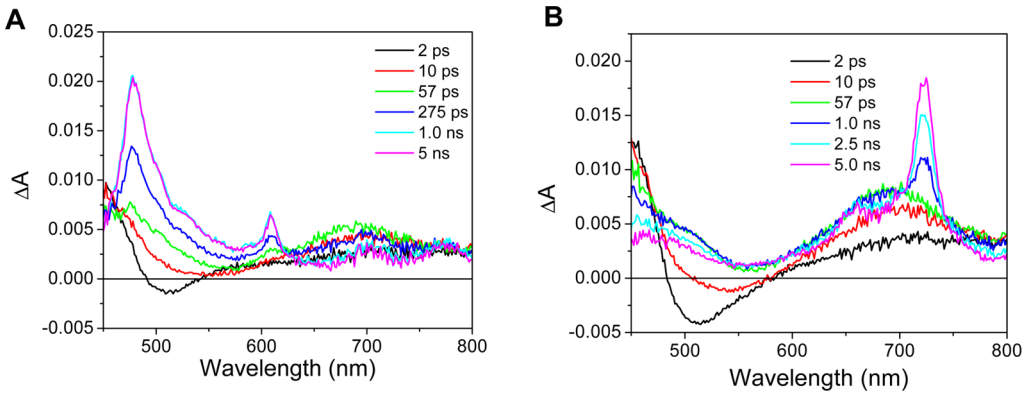

Figure 2. Femtosecond transient absorption spectra of (A) **3B** and (B) **6B** at the indicated times following a 130-fs, 416-nm laser pulse at 295 K.

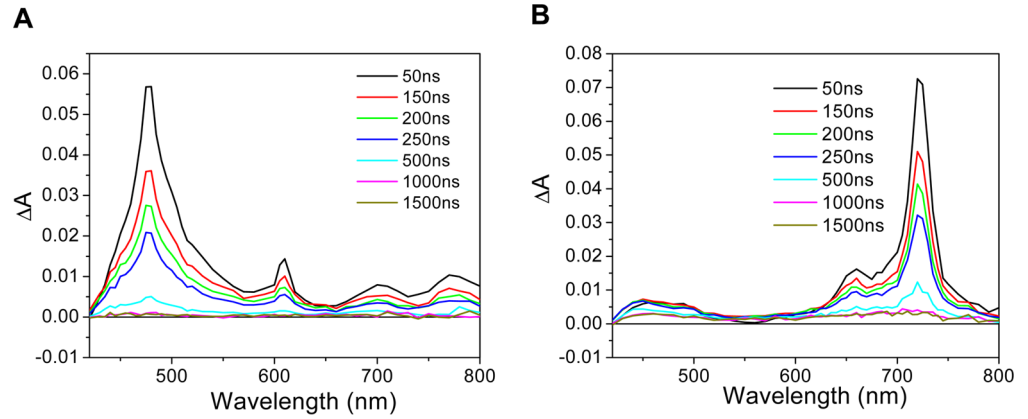

Figure 3. Nanosecond transient absorption spectra of (A) **3B** and (B) **6B** at the indicated times following a 7-ns, 416-nm laser pulse at 295 K.

process, where D−^{1}*C−A−(R$^\bullet$) → D$^{+\bullet}$−C−$^{-\bullet}$−A−(R$^\bullet$) → D$^{+\bullet}$−C−A$^{-\bullet}$−(R$^\bullet$). The transient optical spectra of **1** and **4** were described in detail previously, and their charge separation and recombination time constants are summarized in Table 2.[39,49] Representative transient absorption spectra for **3B** and **6B** are shown in Figure 2, with the time constants for **1A**−**6A** and **1B**−**6B** summarized in Table 2. The presence of R$^\bullet$ has a small or negligible effect on the charge separation time constants. On the other hand, as we reported previously, the presence of R$^\bullet$ changes the charge recombination time constants somewhat.[49] To probe the effect of R$^\bullet$ on the charge recombination time constant, nanosecond transient absorption spectra of **1A**,**B**−**6A**,**B** were acquired in toluene, and representative spectra for **3B** and **6B** are shown in Figure 3. Small to negligible differences in the charge recombination time constants were observed, with the largest change being a factor of 2.5 for **1A** versus **1B** (Table 2).[49]

TREPR Spectroscopy. The steady-state EPR spectra of R$^\bullet$ in **1B**−**6B** (Figure S1, Supporting Information) exhibit three lines due to the 1.5 mT nitrogen hyperfine splitting, whereas proton splittings from the four methyl groups are negligible, indicating that the unpaired spin is localized primarily on the nitrogen and oxygen atoms.

TREPR spectroscopy was utilized to examine the spin dynamics in **1A**,**B**−**6A**,**B**. Panels A and B of Figure 4 show the TREPR spectra of the **2A**−**6A** at 295 and 85 K, respectively,

dx.doi.org/10.1021/jp4045012 | J. Phys. Chem. A 2013, 117, 5314−5325

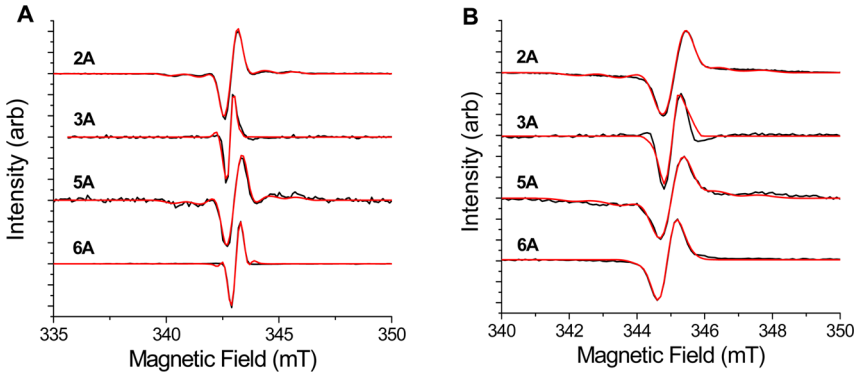

Figure 4. TREPR spectra of **2A**−**6A** 150 ns after a 7-ns, 416-nm laser pulse at (A) 295 and (B) 85 K. Simulations are shown in red.

which display a spin-correlated RP consisting of two emissive and two absorptive transitions superimposed on one another. These spectra are very similar to those of **1A**, which were reported earlier.[35,61] Simulations of the RP spectra using the method of Till and Hore[56] and employing both the g factors and hyperfine splittings of $D^{+\bullet}$ and $A^{-\bullet}$ given in the Supporting Information yield $2J_{DA}$ at both 295 and 85 K, whereas d_{DA} is obtained only at 85 K (Table 2).[56] The $2J_{DA}$ value decreases at 85 K due to the restriction of torsional motion of the 2,5-dimethylphenyl group connecting C and the NI or PI acceptor, as well as freezing out motions of the piperazine ring, and has been observed in similar systems.[62] Panels A and B of Figure 5 show the TREPR spectra of **1B**−**6B** at 295 K in toluene at 100 and 400 ns, respectively, after the laser pulse along with their simulations. At 100 ns, the spectra are dominated by the RP spectra, but at 400 ns, they clearly exhibit three lines matching the hyperfine splitting of $R^{\bullet}$, which are emissive for **1B**−**5B** and absorptive for **6B**, superimposed on the RP signal. No significant change in the RP line shape was found in the presence of $R^{\bullet}$ compared to **1A**−**6A**, so that $2J_{DA}$ within the **1B**−**6B** photogenerated RPs should be approximately the same, as confirmed at 295 K by simulations (Table 2). The TREPR spectra of **1B**−**6B** at 85 K (Figure S2, Supporting Information) differ from those of **1A**−**6A** at 85 K near center field (345 mT). Molecules **1B**, **4B**, and **5B** display overall emissive $R^{\bullet}$ features with no RP signal, whereas for **2B** and **3B**, an RP signal is also evident. The signal observed for **6B** is almost exclusively due to an RP with only a small contribution from spin-polarized $R^{\bullet}$. These spectra are susceptible to saturation effects as a result of using CW microwaves, so that field-swept electron spin−echo-detected (FS-ED) EPR spectra were used to examine the polarization of $R^{\bullet}$ at 85 K.

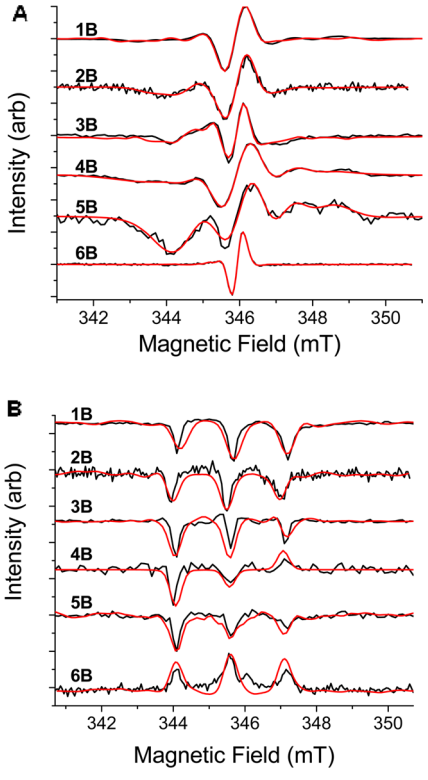

Figure 5. TREPR spectra of **1B**−**6B** (A) 100 and (B) 400 ns following a 7-ns, 416-nm laser pulse at 295 K. Simulations are shown in red.

In addition to the polarized $R^{\bullet}$ and RP signals, a triplet state is observed at 85 K following charge recombination in **1A**,**B**−**3A**,**B** (e.g., see Figure S3 of the Supporting Information for **2B**) with D and E values of 73 and ∼0 mT, respectively, matching those of ^{3}*NI.[63] The ^{3}*NI polarization pattern is (a, e, e, a, a, e), indicating that the triplet is formed by charge recombination of a spin-correlated RP.[5] Although ^{3}*C should be energetically accessible following charge recombination, it was not observed by TREPR spectroscopy. No triplet signal was observed for **4A**,**B**−**6A**,**B**, as expected given that $\Delta G_{RP} \leq E_T$ for the donors and acceptors in these molecules.

The Boltzmann population for electron spins is given by

$$\frac{N_\alpha}{N_\beta} = e^{-\Delta E/k_B T} \tag{9}$$

where N_α and N_β are the numbers of electron spins in the α and β states, respectively; ΔE is the difference in energy (9.5 GHz); k_B is the Boltzmann constant; and T is the temperature. At thermal equilibrium at 85 K and 9.5 GHz, the difference in population between the upper- and lower-energy states is only 0.6%. The FS-ED EPR spectra of **1B**−**6B** at 85 K with no photoexcitation display the well-known g anisotropy of $R^{\bullet}$ (data for **1B** are shown in Figure 6). Unlike the experiments using CW microwaves, photoinitiated FS-ED EPR experiments are sensitive to both the dark Boltzmann spin polarization and the light-induced transient spin polarization of $R^{\bullet}$ and provide a means of quantifying the net light-induced polarization, which is obtained by subtracting the dark FS-ED signal from the photogenerated signal. The light-induced FS-ED TREPR spectra show polarization of $R^{\bullet}$ for **1B**−**6B**, having spectral widths matching those observed with CW microwave detection.

dx.doi.org/10.1021/jp4045012 | J. Phys. Chem. A 2013, 117, 5314−5325

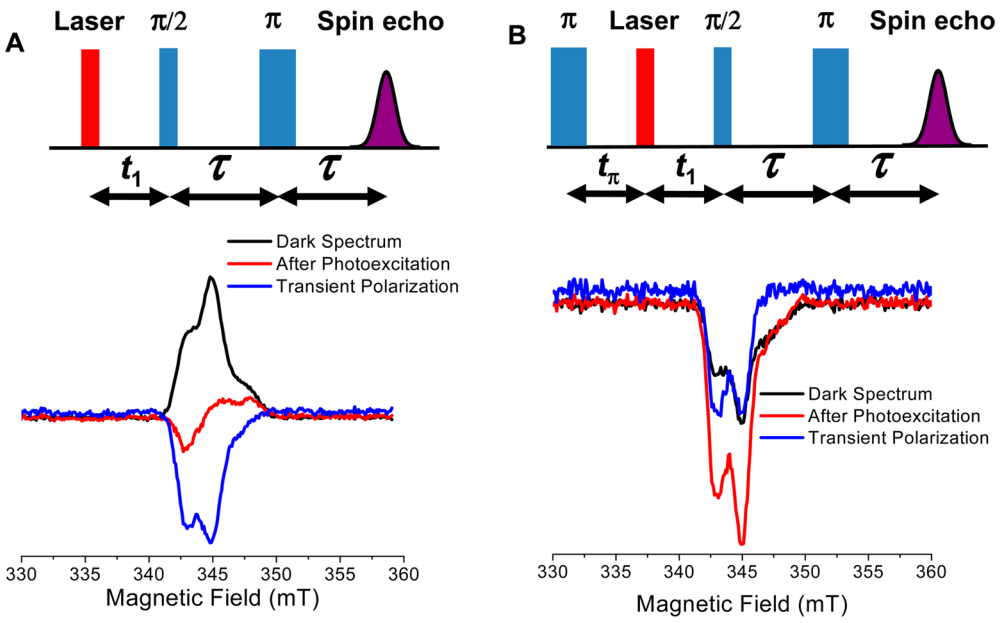

Figure 6. Field-swept echo-detected (FS-ED) spectra of **1B** at 85 K using the pulse sequences shown above the spectra: (A) without and (B) with a π prepulse. A 7-ns, 416-nm laser pulse was used. The other parameters are t_I = 10 ns, t_L = 1 μs, τ = 140 ns, and the $\pi/2$ and π microwave pulses were 12 and 24 ns long, respectively.

Figure 6A shows the TREPR spectrum of **1B** following the pulse sequence (laser−t_L−$\pi/2$−τ−π−τ−echo), where t_L = 1 μs and τ = 140 ns and the $\pi/2$ and π microwave pulses are 12 and 24 ns long, respectively, along with the dark spectrum of R$^\bullet$, which is subtracted from the light-induced spectrum to yield the transient polarization. The corresponding spectra of **2B**−**6B** have similar spectral features and are shown in Figure S4 (Supporting Information). Emissive polarization was observed in **1B**, **2B**, and **4B** 1 μs after the laser pulse, whereas absorptive polarization was observed in **3B**, **5B**, and **6B** 20 μs after the laser pulse, which is consistent with the room-temperature TREPR results using CW microwaves described earlier. The light-induced polarization of R$^\bullet$ decays with the spin−lattice relaxation time of R$^\bullet$ at 85 K, which is ∼25 μs.[64]

By varying the donor and acceptor, we examined the influence of $2J_{DA}$, d_{DA}, and the presence or absence of a triplet state formed by charge recombination on the polarization mechanism. However, the effect of the intrinsic Boltzmann spin population of R$^\bullet$ on the light-induced polarization can also be tested by applying a microwave π pulse prior to photoexcitation to invert the intrinsic spin polarization of R$^\bullet$, followed by the same echo detection sequence as described previously. The data were obtained with the pulse sequence (π−t_I−laser−t_L−$\pi/2$−τ−π−τ−echo), where t_I = 10 ns and the remaining parameters are the same as described for the dark experiment. The data for **1B** are shown in Figure 6B, whereas those for **2B**−**6B** are given in Figure S5 (Supporting Information). The data show that the dark spectra of R$^\bullet$ in **1B**−**6B** are efficiently inverted by application of the π microwave pulse and that the light-induced polarization has the same sign (emissive or absorptive) as the spectra without a π inversion pulse along with similar magnitudes. Using this pulse sequence, it was possible to determine that the magnitude of the transient polarization varies significantly with $|2J_{DA}|$, with **1B**−**6B** having 105%, 10%, 2%, 85%, 4%, and 1% transient polarization, respectively, relative to the Boltzmann polarization of the dark-state signal.

DISCUSSION

Transient Optical Absorption Spectroscopy. The charge separation time constants for **1A**−**6A** are very similar to those observed in **1B**−**6B**, indicating that R$^\bullet$ has minimal influence on the charge separation time constants in **1B**−**6B**, which is consistent with previous observations.[47,49,50] This is likely due to the fast charge separation relative to the spin motion of D$^{+\bullet}$, A$^{-\bullet}$, and R$^\bullet$, along with the very weak electronic coupling between ^{1}*C and R$^\bullet$. The charge separation time constants for the second charge separation step are significantly slower in **4A**,**B**−**6A**,**B** compared to **1A**,**B**−**3A**,**B** as a result of PI being more difficult to reduce than NI,[65] which decreases the free energy of the secondary charge separation reaction. The charge recombination time constants in **1B** and **4B** relative to those of **1A** and **4A**, respectively, are altered by at most a factor of 2.5 by the presence of R$^\bullet$,[48,49] whereas those of **2B**, **3B**, **5B**, and **6B** are not changed significantly (<10%) relative to the corresponding molecules without R$^\bullet$. The charge recombination time constant is primarily determined by the free energy of reaction and the electronic coupling matrix element, V_{DA}^2, for charge recombination, the latter of which is proportional to $2J_{DA}$.[23] As reported earlier, the presence of R$^\bullet$ does not change the reduction potential of NI and PI,[47,49] so that the driving force for the electron-transfer reactions should not change. Although $2J_{DA}$ within the RP changes slightly in the presence of a third spin,[47,49] we did not see significant changes in $2J_{DA}$ in **2B**, **3B**, **5B**, and **6B** by TREPR spectroscopy relative to the corresponding molecules without R$^\bullet$, consistent with the small change in the observed charge recombination time constant with R$^\bullet$ appended.

TREPR Spectroscopy. Three possible mechanisms could be responsible for the spin polarization observed on R$^\bullet$: (i) interaction of R$^\bullet$ with ^{3}*NI or ^{3}*PI, (ii) the influence of $2J_{AR}$ and d_{AR} between NI$^{-\bullet}$ or PI$^{-\bullet}$ and R$^\bullet$, and (iii) polarization transfer from the spin-correlated RP to R$^\bullet$. The mechanism responsible for the observed spin polarization in **1B**−**6B** also

dx.doi.org/10.1021/jp4045012 | J. Phys. Chem. A 2013, 117, 5314−5325

needs to account for the line shape differences in $R^{\bullet}$ and the dependence of the transient polarization magnitude on $|2J_{DA}|$.

We first consider the interaction of $R^{\bullet}$ with ^{3}*NI or ^{3}*PI, where the Hamiltonian for three-spin mixing in a triplet radical system is given by

$$\mathcal{H} = \mathcal{H}_Z + \mathcal{H}_{HF} + \mathcal{H}_D + \mathcal{H}_{EX} = g_T\beta_e B_0 \mathbf{S}^T{}_Z + g_R\beta_e B_0 \mathbf{S}^R{}_Z + \sum_i \mathbf{S}^R\cdot\mathbf{A}\cdot\mathbf{I}_i^R + \mathbf{S}^T\cdot\mathbf{D}_T\cdot\mathbf{S}^T + \mathbf{S}^T\cdot\mathbf{D}_{TR}\cdot\mathbf{S}^R + 2J_{TR}\mathbf{S}^T\cdot\mathbf{S}^R \quad (10)$$

where β_e is the Bohr magneton; g_T and g_R are the g values for the triplet and ground-state radical, respectively; B_0 is the applied magnetic field; $\mathbf{A}$ is the hyperfine tensor; $\mathbf{S}$ and $\mathbf{I}$ are the electron and nuclear spin operators, respectively; $\mathbf{D}$ is the dipolar tensor; and $2J_{TR}$ is the exchange interaction between the electron on $R^{\bullet}$ and the two electrons on ^{3}*NI or ^{3}*PI. When $|2J_{TR}|$ is larger than the other magnetic interactions (strong-exchange regime), the exchange interaction removes the spin degeneracy, resulting in the formation of excited doublet and quartet states.[66] In the strong-exchange regime, the g factors of the excited doublet (g_D) and quartet (g_Q) states should be linear combinations of those of the ground-state doublet (g_R) and excited triplet (g_T) states, according to eqs 11 and 12,[66] whereas the hyperfine splittings, a_N, should follow eqs 13 and 14. The zero-field splitting parameters for a quartet state are different from those of a triplet state and obey eq 15, where D_Q is the zero-field splitting of the quartet state, D_T is the zero-field splitting of the triplet state, and D_{TR} is the dipolar interaction between the electrons on $R^{\bullet}$ and the two electrons on ^{3}*NI or ^{3}*PI. In the weak-exchange limit, the EPR spectrum should show separate resonances for the triplet and ground-state radical with the corresponding g factor and hyperfine splitting.

$$g_D = -\frac{1}{3}g_R + \frac{4}{3}g_T \quad (11)$$

$$g_Q = \frac{1}{3}g_R + \frac{2}{3}g_T \quad (12)$$

$$a_N^D = -\frac{1}{3}a_N^R \quad (13)$$

$$a_N^Q = \frac{1}{3}a_N^R \quad (14)$$

$$D_Q = \frac{1}{3}(D_T + D_{TR}) \quad (15)$$

Equations 13 and 14 predict that the hyperfine splitting of a quartet or doublet state should be one-third that of the ground state. The hyperfine splitting of the polarized $R^{\bullet}$ signal observed at room temperature matches the steady-state hyperfine splitting of $R^{\bullet}$, and thus, the signal is assigned to the $R^{\bullet}$ ground-state doublet. Although the spectral width of the transient signal at 85 K is slightly smaller than that of the $R^{\bullet}$ doublet ground state, it is substantially larger than that predicted by eqs 13 and 14, indicating that excited quartet and doublet states are not responsible for the signal observed at the center of the spectrum at either 295 or 85 K. The triplet spectrum observed at 85 K matches the zero-field splitting parameters of ^{3}*NI, indicating that the spin−spin interaction between ^{3}*NI and $R^{\bullet}$ is weak, providing further evidence that a quartet state is not present. It is possible that the observed spin polarization of $R^{\bullet}$ could be due to radical−triplet interactions that are in the weak-exchange regime; however, $R^{\bullet}$ is still polarized in **4B−6B** even though ^{3}*PI is energetically inaccessible from the charge-separated state. Although charge recombination could produce ^{3}*C, its spin−spin exchange interaction with $R^{\bullet}$ is expected to be very small because of the long distance between them. Furthermore, the involvement of ^{3}*C would not explain the variations in the degree of polarization observed with the different donors.

Next, we address the possibility that the polarization is due to the exchange and/or dipolar interactions between $R^{\bullet}$ and $NI^{-\bullet}$ or $PI^{-\bullet}$, respectively. These interactions could be large because of the short distance between the radical anion and $R^{\bullet}$. However, this explanation is again inconsistent with the varying degrees of polarization observed with different donors because the exchange and dipolar interactions between $R^{\bullet}$ and $NI^{-\bullet}$ or $PI^{-\bullet}$ should not depend on the donor used.

Numerous systems have been designed to explore how the donor−acceptor electronic coupling matrix element (V_{DA}), where $2J_{DA} \propto V_{DA}{}^2$, affects the photophysics and spin dynamics of D−B−A molecules.[22,23,31,41] Changing V_{DA} in D−B−A systems is typically accomplished by varying the distance between the donor and acceptor, which unfortunately also changes $2J_{DA}$ and d_{DA} because both are distance-dependent. To date, only one D−B−A system has been reported in which the donor and acceptor distance (and therefore d_{DA}) is kept constant and $2J_{DA}$ is altered by varying the electronic structure of $D^{+\bullet}$−B−$A^{-\bullet}$.[67] The measured values of $2J_{DA}$ for molecules **1**−**6** decrease in the order **1**, **4** > **2**, **5** ≫ **3**, **6**, which results from differences in the spin density distributions $MeOAn^{+\bullet}$, $DioxAn^{+\bullet}$, and $BDXAn^{+\bullet}$. Unrestricted B3LYP DFT calculations at the 6-31G(d) level of theory show a general shift in the spin density distribution onto the progressively more oxygenated phenyl rings of the donor cation radicals (see the Supporting Information), thus slightly increasing the average distance between the two unpaired electrons in the charge-separated state, which changes both $2J_{DA}$ and d_{DA}. However, $2J_{DA}$ is much more sensitive to small distance (r) changes because $2J_{DA} \propto e^{-r}$ whereas $d_{DA} \propto 1/r^3$.

Polarization transfer from the weakly spin−spin exchange-coupled photogenerated RP to the $R^{\bullet}$ observer spin appears to be the model most consistent with our results.[44,45] The magnitude of the transient polarization observed following the application of a π pulse is the same as that observed without initially inverting the spin sublevel population of $R^{\bullet}$. This indicates that the initial Boltzmann population of the spin sublevels does not affect the observed light-induced spin polarization and that the light-induced polarization on $R^{\bullet}$ comes from spin mixing with the photogenerated RP.

Although both $2J_{DA}$ and d_{DA} depend on the RP distance, one can determine whether $2J_{DA}$ or d_{DA} is exclusively responsible for the observed polarization by comparing the results obtained in liquid and solid solution. As mentioned previously, d_{DA} is inherently anisotropic and should be averaged to essentially zero in liquid solution, whereas $2J_{DA}$ is isotropic under all conditions, meaning that $2J_{DA}$ should account exclusively for the polarization observed in liquid solution at 295 K. Moreover, as noted previously, $d_{DA} \propto 1/r^3$ whereas $2J_{DA} \propto e^{-r}$, so that the relatively small D−A distance changes in **1A,B**−**6A,B** result in d_{DA} remaining nearly constant, whereas $2J_{DA}$ varies by 1−2 orders of magnitude in the two series **1A,B**−**3A,B** and **4A,B**−**6A,B** (Table 2).

dx.doi.org/10.1021/jp4045012 | J. Phys. Chem. A 2013, 117, 5314−5325

Finally, a word about the sign of the polarization transferred from $D^{+\bullet}-C-A^{-\bullet}$ to $R^{\bullet}$. When $k_T > k_S$, the polarization of the observer spin will correspond to that of the triplet subensemble of the RP, whereas when $k_S > k_T$, the observer spin inherits the polarization from the singlet subensemble of the RP. Salikhov et al.[44] presented an analytical expression that yields the sign of the net polarization transfer to the observer spin when $k_S \neq k_T$ using second-order perturbation theory

$$\Gamma_2 = \text{sign}\left[\left(\frac{k_T - k_S}{k_T + k_S}\right)(A_{DR^{\bullet}} - A_{AR^{\bullet}})(\omega_D - \omega_A)\right] \quad (16)$$

where the variables were defined previously. If Γ_2 is positive, the EPR spectrum of $R^{\bullet}$ will be emissive, whereas if Γ_2 is negative, the EPR spectrum of $R^{\bullet}$ will be absorptive. If, on the other hand, $k_T \approx k_S$, Salikhov et al.[44] found that a fourth-order perturbation theory expression is necessary to capture the sign of the net polarization transfer from $D^{+\bullet}-C-A^{-\bullet}$ to $R^{\bullet}$

$$\Gamma_4 = \text{sign}\left[-\frac{(2J_{DA} + d_{DA})(\omega_D - \omega_{R^{\bullet}})}{2} + \frac{3d_{DA}(\omega_A - \omega_{R^{\bullet}})}{4}\right] \quad (17)$$

where the variables were defined previously. If Γ_4 is positive, the $R^{\bullet}$ spectrum is emissive, whereas the opposite is true if Γ_4 is negative. It can be seen directly from eqs 16 and 17 that the sign of $2J_{DA}$ and the magnitudes of k_T and k_S relative to one another play dominant roles in determining whether the polarization of $R^{\bullet}$ is emissive or absorptive, especially in liquid solution, where fast molecular tumbling averages out all anisotropic interactions. In contrast, in low-temperature glassy media, the anisotropies of all of the magnetic parameters must be taken into account, so that predicting the sign of the polarization from a simple perturbation theory expression is difficult, and it is best to rely on the full simulation based on the Liouville equation.

CONCLUSIONS

We have shown that the charge separation rates for rapid photogeneration of a spin-correlated RP do not change significantly in the presence of the stable radical. We have also shown that the subsequent charge recombination is accompanied by spin polarization transfer from the RP to $R^{\bullet}$ and that the degree of polarization transferred to $R^{\bullet}$ depends on $|2J_{DA}|$. At the same time, the degree of spin polarization transfer does not depend on the presence of ^{3}*A resulting from charge recombination. The spin relaxation time of $R^{\bullet}$ is about 2 orders of magnitude longer than that of the spin-polarized RP, thus providing a means to store photogenerated spin polarization, which might have applications in organic spintronic devices.

ASSOCIATED CONTENT

Supporting Information

Experimental details, including synthesis, and additional transient absorption and TREPR data. This material is available free of charge via the Internet at http://pubs.acs.org.

AUTHOR INFORMATION

Corresponding Author

*E-mail: m-wasielewski@northwestern.edu.

Notes

The authors declare no competing financial interest.

ACKNOWLEDGMENTS

This work was supported by the National Science Foundation under Grant CHE-1012378. M.T.C. thanks the Link Foundation for a fellowship. D.M.G. thanks the NDSEG for a graduate fellowship. M.A.R. acknowledges support from DARPA under Award N66001-10-1-4066. R.C. (EPR analysis) was supported as part of the ANSER Center, an Energy Frontier Research Center funded by the U.S. Department of Energy (DOE), Office of Science, Office of Basic Energy Sciences, under Award DE-SC0001059.

REFERENCES

(1) Rajca, A. The Physical Organic Chemistry of Very High-Spin Polyradicals. *Adv. Phys. Org. Chem.* **2005**, *40*, 153−199.
(2) Epstein, A. J. Organic-Based Magnets. Opportunities in Photoinduced Magnetism, Spintronics, Fractal Magnetism, and Beyond. *MRS Bull.* **2003**, *28*, 492−499.
(3) Awschalom, D. D.; Flatte, M. E.; Samarth, N. Microelectronic Devices That Function by Using the Spin of the Electron Are a Nascent Multibillion-Dollar Industry—and May Lead to Quantum Microchips. *Sci. Am.* **2002**, *286*, 67−73.
(4) Wolf, S. A.; Awschalom, D. D.; Buhrman, R. A.; Daughton, J. M.; von Molnar, S.; Roukes, M. L.; Chtchelkanova, A. Y.; Treger, D. M. Spintronics: A Spin-Based Electronics Vision for the Future. *Science* **2001**, *294*, 1488−1495.
(5) Levanon, H.; Norris, J. R. The Photoexcited Triplet State and Photosynthesis. *Chem. Rev.* **1978**, *78*, 185−198.
(6) Kawai, A.; Shibuya, K. Electron Spin Dynamics in a Pair Interaction between Radical and Electronically-Excited Molecule as Studied by a Time-Resolved ESR Method. *J. Photochem. Photobiol. C* **2006**, *7*, 89−103.
(7) Blank, A.; Levanon, H. Triplet Radical Interaction. Direct Measurement of Triplet Polarization Transfer by Fourier Transform Electron Paramagnetic Resonance. *J. Phys. Chem. A* **2000**, *104*, 794−800.
(8) Blank, A.; Levanon, H. Interaction between Polarized Triplets and Stable Radicals in Liquid Solutions. *J. Phys. Chem. A* **2001**, *105*, 4799−4807.
(9) Franco, L.; Mazzoni, M.; Corvaja, C.; Gubskaya, V. P.; Berezhnaya, L. S.; Nuretdinov, I. A. TR-EPR of Single and Double Spin Labelled C_{60} Derivatives: Observation of Quartet and Quintet Excited States in Solution. *Mol. Phys.* **2006**, *104*, 1543−1550.
(10) Fujisawa, J.; Ishii, K.; Ohba, Y.; Yamauchi, S.; Fuhs, M.; Möbius, K. First Observation of the Excited Doublet State of a Radical-Triplet Pair in Solution: W-Band High-Field Time-Resolved Electron Paramagnetic Resonance Spectroscopy. *J. Phys. Chem. A* **1999**, *103*, 213−216.
(11) Rozenshtein, V.; Berg, A.; Stavitski, E.; Levanon, H.; Franco, L.; Corvaja, C. Electron Spin Polarization of Functionalized Fullerenes. Reversed Quartet Mechanism. *J. Phys. Chem. A* **2005**, *109*, 11144−11154.
(12) Sartori, E.; Toffoletti, A.; Corvaja, C.; Garlaschelli, L. Electron Spin Polarization Transfer and Radical-Triplet Pair Polarization in Nitroxide−C_{60} Derivative Systems. *J. Phys. Chem. A* **2001**, *105*, 10776−10780.
(13) Fujisawa, J.; Ishii, K.; Ohba, Y.; Yamauchi, S.; Fuhs, M.; Möbius, K. X- and W-Band Time-Resolved Electron Paramagnetic Resonance Studies on Radical-Excited Triplet Pairs between Metalloporphyrins and Axial-Ligating Nitroxide Radicals. *J. Phys. Chem. A* **1997**, *101*, 5869−5876.
(14) Colvin, M. T.; Giacobbe, E. M.; Cohen, B.; Miura, T.; Scott, A. M.; Wasielewski, M. R. Competitive Electron Transfer and Enhanced Intersystem Crossing in Photoexcited Covalent TEMPO−Perylene-3,4:9,10-bis(dicarboximide) Dyads: Unusual Spin Polarization Result-

ing from the Radical-Triplet Interaction. *J. Phys. Chem. A* **2010**, *114*, 1741−1748.
(15) Colvin, M. T.; Ricks, A. B.; Scott, A. M.; Smeigh, A. L.; Carmieli, R.; Miura, T.; Wasielewski, M. R. Magnetic Field-Induced Switching of the Radical-Pair Intersystem Crossing Mechanism in a Donor−Bridge−Acceptor Molecule for Artificial Photosynthesis. *J. Am. Chem. Soc.* **2011**, *133*, 1240−1243.
(16) Colvin, M. T.; Smeigh, A. L.; Giacobbe, E. M.; Conron, S. M. M.; Ricks, A. B.; Wasielewski, M. R. Ultrafast Intersystem Crossing and Spin Dynamics of Zinc *meso*-Tetraphenylporphyrin Covalently Bound to Stable Radicals. *J. Phys. Chem. A* **2011**, *115*, 7538−7549.
(17) Giacobbe, E. M.; Mi, Q. X.; Colvin, M. T.; Cohen, B.; Ramanan, C.; Scott, A. M.; Yeganeh, S.; Marks, T. J.; Ratner, M. A.; Wasielewski, M. R. Ultrafast Intersystem Crossing and Spin Dynamics of Photoexcited Perylene-3,4:9,10-bis(dicarboximide) Covalently Linked to a Nitroxide Radical at Fixed Distances. *J. Am. Chem. Soc.* **2009**, *131*, 3700−3712.
(18) Teki, Y.; Toichi, T.; Nakajima, S. π Topology and Spin Alignment in Unique Photoexcited Triplet and Quintet States Arising from Four Unpaired Electrons of an Organic Spin System. *Chem.—Eur. J.* **2006**, *12*, 2329−2336.
(19) Hasharoni, K.; Levanon, H.; Greenfield, S. R.; Gosztola, D. J.; Svec, W. A.; Wasielewski, M. R. Mimicry of the Radical Pair and Triplet States in Photosynthetic Reaction Centers with a Synthetic Model. *J. Am. Chem. Soc.* **1995**, *117*, 8055−8056.
(20) Carbonera, D.; Di Valentin, M.; Corvaja, C.; Agostini, G.; Giacometti, G.; Liddell, P. A.; Kuciauskas, D.; Moore, A. L.; Moore, T. A.; Gust, D. EPR Investigation of Photoinduced Radical Pair Formation and Decay to a Triplet State in a Carotene−Porphyrin−Fullerene Triad. *J. Am. Chem. Soc.* **1998**, *120*, 4398−4405.
(21) Shaakov, S.; Galili, T.; Stavitski, E.; Levanon, H.; Lukas, A.; Wasielewski, M. R. Using Spin Dynamics of Covalently Linked Radical Ion Pairs to Probe the Impact of Structural and Energetic Changes on Charge Recombination. *J. Am. Chem. Soc.* **2003**, *125*, 6563−6572.
(22) Weiss, E. A.; Ratner, M. A.; Wasielewski, M. R. Direct Measurement of Singlet−Triplet Splitting within Rodlike Photogenerated Radical Ion Pairs Using Magnetic Field Effects: Estimation of the Electronic Coupling for Charge Recombination. *J. Phys. Chem. A* **2003**, *107*, 3639−3647.
(23) Weiss, E. A.; Ahrens, M. J.; Sinks, L. E.; Gusev, A. V.; Ratner, M. A.; Wasielewski, M. R. Making a Molecular Wire: Charge and Spin Transport through *para*-Phenylene Oligomers. *J. Am. Chem. Soc.* **2004**, *126*, 5577−5584.
(24) Weiss, E. A.; Tauber, M. J.; Kelley, R. F.; Ahrens, M. J.; Ratner, M. A.; Wasielewski, M. R. Conformationally Gated Switching between Superexchange and Hopping within Oligo-*p*-phenylene-Based Molecular Wires. *J. Am. Chem. Soc.* **2005**, *127*, 11842−11850.
(25) Dance, Z. E. X.; Mi, Q.; McCamant, D. W.; Ahrens, M. J.; Ratner, M. A.; Wasielewski, M. R. Time-Resolved EPR Studies of Photogenerated Radical Ion Pairs Separated by *p*-Phenylene Oligomers and of Triplet States Resulting from Charge Recombination. *J. Phys. Chem. B* **2006**, *110*, 25163−25173.
(26) Closs, G. L.; Forbes, M. D. E.; Norris, J. R. Spin-Polarized Electron Paramagnetic Resonance Spectra of Radical Pairs in Micelles: Observation of Electron Spin−Spin Interactions. *J. Phys. Chem.* **1987**, *91*, 3592−3599.
(27) Hore, P. J.; Hunter, D. A.; Mckie, C. D.; Hoff, A. J. Electron Paramagnetic Resonance of Spin-Correlated Radical Pairs in Photosynthetic Reactions. *Chem. Phys. Lett.* **1987**, *137*, 495−500.
(28) Steiner, U. E.; Ulrich, T. Magnetic Field Effects in Chemical Kinetics and Related Phenomena. *Chem. Rev.* **1989**, *89*, 51−147.
(29) Miura, T.; Scott, A. M.; Wasielewski, M. R. Electron Spin Dynamics as a Controlling Factor for Spin-Selective Charge Recombination in Donor−Bridge−Acceptor Molecules. *J. Phys. Chem. C* **2010**, *114*, 20370−20379.
(30) Weiss, E. A.; Wasielewski, M. R.; Ratner, M. A. A General Formulation for Magnetic Exchange Coupling within Long-Distance Radical Ion Pairs. *J. Chem. Phys.* **2005**, *123*, 064504-1−064504-8.
(31) Kobori, Y.; Sekiguchi, S.; Akiyama, K.; Tero-Kubota, S. Chemically Induced Dynamic Electron Polarization Study on the Mechanism of Exchange Interaction in Radical Ion Pairs Generated by Photoinduced Electron Transfer Reactions. *J. Phys. Chem. A* **1999**, *103*, 5416−5424.
(32) Wasielewski, M. R.; Bock, C. H.; Bowman, M. K.; Norris, J. R. Controlling the Duration of Photosynthetic Charge Separation with Microwave Radiation. *Nature* **1983**, *303*, 520−522.
(33) Murai, H. Spin-Chemical Approach to Photochemistry: Reaction Control by Spin Quantum Operation. *J. Photochem. Photobiol. C* **2003**, *3*, 183−201.
(34) van Dijk, B.; Gast, P.; Hoff, A. J.; Dzuba, S. A. Control of Singlet-Precursor Radical Pair Lifetime by Manipulation of Spin-Selective Reaction Pathways. *J. Phys. Chem. A* **1997**, *101*, 719−724.
(35) Hasharoni, K.; Levanon, H.; Greenfield, S. R.; Gosztola, D. J.; Svec, W. A.; Wasielewski, M. R. Radical Pair and Triplet State Dynamics of a Photosynthetic Reaction-Center Model Embedded in Isotropic Media and Liquid Crystals. *J. Am. Chem. Soc.* **1996**, *118*, 10228−10235.
(36) Kobori, Y.; Yamauchi, S.; Akiyama, K.; Tero-Kubota, S.; Imahori, H.; Fukuzumi, S.; Norris, J. R., Jr. Primary Charge-Recombination in an Artificial Photosynthetic Reaction Center. *Proc. Natl. Acad. Sci. U.S.A.* **2005**, *102*, 10017−10022.
(37) Hore, P. J. In *Advanced EPR in Biology and Biochemistry*; Hoff, A. J., Ed.; Elsevier: Amsterdam, 1989; pp 405−440.
(38) Levanon, H.; Hasharoni, K. Electron and Energy Transfer in Liquid Crystals. Time-Resolved Electron Paramagnetic Resonance. *Prog. React. Kinet.* **1995**, *20*, 309−346.
(39) Carmieli, R.; Mi, Q. X.; Ricks, A. B.; Giacobbe, E. M.; Mickley, S. M.; Wasielewski, M. R. Direct Measurement of Photoinduced Charge Separation Distances in Donor−Acceptor Systems for Artificial Photosynthesis Using OOP-ESEEM. *J. Am. Chem. Soc.* **2009**, *131*, 8372−8373.
(40) Scott, A. M.; Miura, T.; Ricks, A. B.; Dance, Z. E. X.; Giacobbe, E. M.; Colvin, M. T.; Wasielewski, M. R. Spin-Selective Charge Transport Pathways through *p*-Oligophenylene-Linked Donor−Bridge−Acceptor Molecules. *J. Am. Chem. Soc.* **2009**, *131*, 17655−17666.
(41) Scott, A. M.; Ricks, A. B.; Colvin, M. T.; Wasielewski, M. R. Comparing Spin-Selective Charge Transport through Donor−Bridge−Acceptor Molecules with Different Oligomeric Aromatic Bridges. *Angew. Chem., Int. Ed.* **2010**, *49*, 2904−2908.
(42) Hoff, A. J.; Hore, P. J. Electron Spin Polarization in a Three-Electron Spin System. An Application to Bacterial Photosynthesis. *Chem. Phys. Lett.* **1984**, *108*, 104−110.
(43) Hore, P. J.; Riley, D. J.; Semlyen, J. J.; Zwanenburg, G.; Hoff, A. J. Analysis of Anisotropic Electron Spin Polarization in the Photosynthetic Bacterium *Rhodospirillum rubrum*. Evidence That the Sign of the Exchange Interaction in the Primary Radical Pair Is Positive. *Biochim. Biophys. Acta, Bioenerg.* **1993**, *1141*, 221−230.
(44) Salikhov, K. M.; Van der Est, A. J.; Stehlik, D. The Transient EPR Spectra and Spin Dynamics of Coupled Three-Spin Systems in Photosynthetic Reaction Centers. *Appl. Magn. Reson.* **1999**, *16*, 101−134.
(45) Salikhov, K. M.; Zech, S. G.; Stehlik, D. Light Induced Radical Pair Intermediates in Photosynthetic Reaction Centres in Contact with an Observer Spin Label: Spin Dynamics and Effects on Transient EPR Spectra. *Mol. Phys.* **2002**, *100*, 1311−1321.
(46) Blankenship, R. E. *Molecular Mechanisms of Photosynthesis*; Blackwell Science: Oxford, U.K., 2002.
(47) Weiss, E. A.; Chernick, E. T.; Wasielewski, M. R. Modulation of Radical Ion Pair Lifetimes by the Presence of a Third Spin in Rodlike Donor−Acceptor Triads. *J. Am. Chem. Soc.* **2004**, *126*, 2326−2327.
(48) Chernick, E. T.; Mi, Q.; Kelley, R. F.; Weiss, E. A.; Jones, B. A.; Marks, T. J.; Ratner, M. A.; Wasielewski, M. R. Electron Donor−Bridge−Acceptor Molecules with Bridging Nitronyl Nitroxide Radicals: Influence of a Third Spin on Charge- and Spin-Transfer Dynamics. *J. Am. Chem. Soc.* **2006**, *128*, 4356−4364.

(49) Mi, Q.; Chernick, E. T.; McCamant, D. W.; Weiss, E. A.; Ratner, M. A.; Wasielewski, M. R. Spin Dynamics of Photogenerated Triradicals in Fixed Distance Electron Donor−Chromophore−Acceptor−TEMPO Molecules. *J. Phys. Chem. A* **2006**, *110*, 7323−7333.
(50) Chernick, E. T.; Mi, Q.; Vega, A. M.; Lockard, J. V.; Ratner, M. A.; Wasielewski, M. R. Controlling Electron Transfer Dynamics in Donor−Bridge−Acceptor Molecules by Increasing Unpaired Spin Density on the Bridge. *J. Phys. Chem. B* **2007**, *111*, 6728−6737.
(51) Teki, Y.; Tamekuni, H.; Takeuchi, J.; Miura, Y. First Evidence for a Uniquely Spin-Polarized Quartet Photoexcited State of a π-Conjugated Spin System Generated via the Ion-Pair State. *Angew. Chem., Int. Ed.* **2006**, *45*, 4666−4670.
(52) Teki, Y.; Tamekuni, H.; Haruta, K.; Takeuchi, J.; Miura, Y. Design, Synthesis, and Uniquely Electron-Spin-Polarized Quartet Photo-Excited State of a π-Conjugated Spin System Generated via the Ion-Pair State. *J. Mater. Chem.* **2008**, *18*, 381−391.
(53) Teki, Y.; Matsumoto, T. Theoretical Study of Dynamic Electron-Spin-Polarization via the Doublet−Quartet Quantum-Mixed State and Time-Resolved ESR Spectra of the Quartet High-Spin State. *Phys. Chem. Chem. Phys.* **2011**, *13*, 5728−5746.
(54) Ahrens, M. J.; Sinks, L. E.; Rybtchinski, B.; Liu, W.; Jones, B. A.; Giaimo, J. M.; Gusev, A. V.; Goshe, A. J.; Tiede, D. M.; Wasielewski, M. R. Self-Assembly of Supramolecular Light-Harvesting Arrays from Covalent Multi-Chromophore Perylene-3,4:9,10-bis(dicarboximide) Building Blocks. *J. Am. Chem. Soc.* **2004**, *126*, 8284−8294.
(55) *MATLAB*; The MathWorks, Inc.: Natick, MA, 2013.
(56) Till, U.; Hore, P. J. Radical Pair Kinetics in a Magnetic Field. *Mol. Phys.* **1997**, *90*, 289−296.
(57) Greenfield, S. R.; Svec, W. A.; Gosztola, D.; Wasielewski, M. R. Multistep Photochemical Charge Separation in Rod-Like Molecules Based on Aromatic Imides and Diimides. *J. Am. Chem. Soc.* **1996**, *118*, 6767−6777.
(58) Hayes, R. T.; Walsh, C. J.; Wasielewski, M. R. Competitive Electron Transfer from the S_2 and S_1 Excited States of Zinc *meso*-Tetraphenylporphyrin to a Covalently Bound Pyromellitimide: Dependence on Donor−Acceptor Structure and Solvent. *J. Phys. Chem. A* **2004**, *108*, 2375−2381.
(59) *HyperChem*, release 3; Hypercube Inc.: Gainesville, FL, 1994.
(60) Gaines, G. L., III; O'Neil, M. P.; Svec, W. A.; Niemczyk, M. P.; Wasielewski, M. R. Photoinduced Electron Transfer in the Solid State: Rate vs Free Energy Dependence in Fixed-Distance Porphyrin−Acceptor Molecules. *J. Am. Chem. Soc.* **1991**, *113*, 719−721.
(61) Mi, Q.; Ratner, M. A.; Wasielewski, M. R. Time-Resolved EPR Spectra of Spin-Correlated Radical Pairs: Spectral and Kinetic Modulation Results from Electron−Nuclear Hyperfine Interactions. *J. Phys. Chem. A* **2010**, *114*, 162−171.
(62) Carmieli, R.; Zeidan, T. A.; Kelley, R. F.; Mi, Q.; Lewis, F. D.; Wasielewski, M. R. Excited State, Charge Transfer, and Spin Dynamics in DNA Hairpin Conjugates with Perylenediimide Hairpin Linkers. *J. Phys. Chem. A* **2009**, *113*, 4691−4700.
(63) Dance, Z. E. X.; Ahrens, M. J.; Vega, A. M.; Ricks, A. B.; McCamant, D. W.; Ratner, M. A.; Wasielewski, M. R. Direct Observation of the Preference of Hole Transfer over Electron Transfer for Radical Ion Pair Recombination in Donor−Bridge−Acceptor Molecules. *J. Am. Chem. Soc.* **2008**, *130*, 830−832.
(64) Eaton, S. S.; Eaton, G. R. Relaxation Times of Organic Radicals and Transition Metal Ions. *Biol. Magn. Reson.* **2000**, *19*, 29−154.
(65) Gosztola, D.; Niemczyk, M. P.; Svec, W.; Lukas, A. S.; Wasielewski, M. R. Excited Doublet States of Electrochemically Generated Aromatic Imide and Diimide Radical Anions. *J. Phys. Chem. A* **2000**, *104*, 6545−6551.
(66) Bencini, A.; Gatteschi, D. *Electron Paramagnetic Resonance of Exchange Coupled Systems*; Springer-Verlag: Berlin, 1990.
(67) Ricks, A. B.; Solomon, G. C.; Colvin, M. T.; Scott, A. M.; Chen, K.; Ratner, M. A.; Wasielewski, M. R. Controlling Electron Transfer in Donor−Bridge−Acceptor Molecules Using Cross-Conjugated Bridges. *J. Am. Chem. Soc.* **2010**, *132*, 15427−15434.